



# Structural,Electrical And Magnetic Properties Of Gadolinium Doped Manganese Cadmium Nanoferrites

Srilata Michael<sup>1</sup>,Dr. D.Ravinder<sup>a</sup>

1 Research Scholar,Department of Physics,Osmania University, Hyderabad,Telangana,India 500007.  
a Professor (Retd.) ,Department of Physics,Osmania University,Hyderabad,Telangana,India 500007 .

## Highlights

- Pure and Gd<sup>3+</sup>doped MnFe<sub>2</sub>O<sub>4</sub> nanoparticles are successfully synthesized.
- Structural analysis is carried out using x-ray diffraction to identify pure ferrite phases.
- The variation of DC electrical resistivity of ferrite nanoparticles with Arrhenius plots is studied.
- The magnetic properties which include Magnetic Saturation,magnetic Coercivity,Magnetic Retentivity and Bohr magneton of the synthesized gadolinium doped Manganese Cadmium nanoferrites are studied with the effect of increase in the doping concentrations of rare earth ions(Gd<sup>3+</sup>) are studied.

**KeyWords:**GadoliniumdopedManganeseCadmiumnanoferrites,XRD,FTIR,TEM,FESEM,SAED,DC resistivity,VSM,ferrimagnetic,paramagnetic.

## Abstract

The compound chosen for the in depth study of structural,dc electrical and magnetic properties is gadolinium doped Manganese Cadmium nanoferrites ,with chemical formula of Mn<sub>0.3</sub>Cd<sub>0.7</sub>Gd<sub>x</sub>Fe<sub>2-x</sub>O<sub>4</sub> (Gd<sup>3+</sup> is the rare earth metal ion which is used as dopant and the values of x ranges from 0.000,0.005,0.010,0.015,0.020,0.025. For x=0.000, the compound is in its pure form without any doping.) The above mentioned synthesized samples are analyzed and characterized by X-ray diffraction (XRD),Fourier transform Infrared spectroscopy (FTIR), Transmission electron Microscopy (TEM) and vibrating sample magnetometer (VSM). The XRD spectra confirmed the formation of the single -phase cubic spinel structure. The average crystallite size evaluated from XRD data was found to be in the range of 32-36nm and found to be in agreement with the results of TEM. In addition, lattice parameter is found to increase with the rare earth metal ion which in this case of study is (Gd<sup>3+</sup>) substitution. DC electrical resistivity as a function of temperature was studied by using two-probe technique and found to decrease with increase in temperature which reveals the semiconducting nature of the samples.Simultaneously,the dc resistivity analysis has shown the transition of ferrimagnetic nature of the sample to paramagnetic nature at the Curie temperature. The band gap energy with doping of rare earth content is also studied.The soft ferrimagnetic behaviour of the prepared samples is identified from the plots drawn from VSM studies.The soft ferrites have numerous applications that include power supplies,filters switching circuits,Magnetic Resonance Imaging,Antennas,Impedance matching devices,Magnetic Sensors,electric motors and various other applications.

**KeyWords:**GadoliniumdopedManganeseCadmiumnanoferrites,XRD,FTIR,TEM,FESEM,SAED,DC resistivity,VSM,ferrimagnetic,paramagnetic.

## INTRODUCTION

Cubic spinel ferrites have gained prominence and are a subject of research due to the ongoing rise of nanotechnology invading every walk of human life in recent years because of their unique structural, electrical and magnetic properties. Its properties can be utilized in a wide range of applications like transformer cores, Magnetic resonance imaging (MRI), microwave devices, targeted drug delivery, medical diagnosis, gas sensors, storage devices and antibacterial activities [1], [2], [3], Manganese ferrite ( $\text{MnFe}_2\text{O}_4$ ) is one of the spinel-type ferrimagnetic material having versatile nature. It has important characteristics such as high saturation magnetization, low eddy losses, high coercive field and high resistivity [4]. These materials are widely used in the applications, such as the core of switched-mode power supply, inductors and RF transformers [5],[6]. The general formula of spinel ferrite is  $\text{AB}_2\text{O}_4$ . The type of lattice in spinel ferrite is face centered cubic (FCC) lattice in which the metal cations A and B are at tetrahedral and octahedral sites respectively [7]. It is to be noted that the method of preparation of the above mentioned samples plays a significant role in influencing the properties of the chosen nanoferrites and also worth while noting is the dependency of the properties on the composition, morphology, grain size and the distribution of cations over A and B sites and these in turn are influenced by the method of preparation. In order to achieve the desired properties of the Gadolinium doped Manganese Cadmium nanoferrites the method of synthesis chosen is citrate gel auto combustion method. It is so chosen as it is cost effective, yields proportionate compound. The rare earth metal ions which is  $\text{Gd}^{3+}$  ions in the present case drastically change the magnetic properties such as large magnetocrystalline anisotropy, magnetic moment and a high magnetostriction on doping of  $\text{Gd}^{3+}$  ions of high ionic radii at very low temperature due to its localized nature of 4f electrons. The substitution of  $\text{Gd}^{3+}$  ions when doped into the manganese cadmium nanoferrites spinel structure can also bring distortion as well as modifications in the properties [8]. Because of the properties of the samples that can be modified as per the requirements, these materials are used in various applications [9],[10].

To work towards the objective set, the samples of Gd doped  $\text{Mn}_{0.3}\text{Cd}_{0.7}\text{Gd}_x\text{Fe}_{2-x}\text{O}_4$  with  $X=0.00, 0.005, 0.010, 0.015, 0.020, 0.025$  are prepared through citrate gel auto combustion method and sintered at temperatures of  $750^\circ\text{C}$ . Using XRD, FTIR, TEM, FESEM and SAED analysis, the polycrystalline, homogeneous, cubic structure of the nano ferrites synthesized was confirmed. Further to investigate the electrical conductivity of the samples, the method used is two probe method where the pellet form of the sample is placed between two electrodes after being coated with conducting material and the temperature of the furnace is increased upto  $1000^\circ\text{C}$ .

### Results and discussion:

**XRD analysis:** PXRD is a characterization technique used to analyze the crystal structure of materials wherein x-rays from an x-ray source ( $\text{Cu K}\alpha$  radiation of wavelength  $1.5405 \text{ \AA}$ ) are directed towards the sample placed in a sample holder so as to produce diffraction pattern which is detected by a detector that moves around the sample measuring the intensity of the scattered radiation at different angles ( $2\theta$ ).

Using XRD analysis, the average crystallite size of the prepared samples was calculated using Debye-Scherrer's formula

$$D = 0.91\lambda / \beta \cos\theta \text{-----(1)}$$

where D stands for the crystallite size in nm,  $\lambda$  is the wave length of the X-rays used ( $1.5405 \text{ \AA}$ ),  $\beta$  is the full width half maximum (FWHM) and ' $\theta$ ' is the diffraction angle in radians.

The lattice constant 'a' is calculated using the formula,  $a = d\sqrt{h^2 + k^2 + l^2}$  (2) Where 'd' is the inter planer spacing which is obtained from the Bragg's equation,  $n\lambda = 2d\sin\theta$

And  $d = n\lambda / 2\sin\theta$  where  $n=1, 2, 3, \dots$   $\lambda$  is the wave length of the X-rays used ' $\theta$ ' is the angle of diffraction.

The hopping lengths are calculated using the following relations for tetrahedral site ( $d_A$ ) and for octahedral site ( $d_B$ ) which are

$$d_A = 0.25 a\sqrt{3} \text{-----(3a)}$$

$$d_B = 0.25 a\sqrt{2} \text{-----(3b)}$$

The X-ray density,  $d_x$ , was calculated by using the following formula,

$$d_x = nM / a^3 N \text{----- (4)}$$

where n is the number of molecules in a unit cell of spinel lattice ( $n=8$ ), M is the molecular weight of the sample and N is the Avagadro number ( $6.023 \times 10^{23}$  molecules/cc).

The Bulk density,  $d_B$  is calculated by using the formula,

$d_B = \frac{m}{\pi r^2 t}$  (5) where  $m$  is the mass of the pellet,  $r$  is the radius of the pellet and  $t$  is the thickness of the pellet.

The porosity of the sample is determined from the relation ,

$P = \left( \frac{d_x - d_B}{d_x} \right) \times 100$  (6)

where  $d_x$  is the x-ray density and  $d_B$  is the bulk density.

The procedure

followed for the study of dc electrical resistivity which is temperature dependent involves making a pellet form of the sample prepared using hydraulic press and then the pellet is coated with silver paint on both of its surfaces and heated on a hot plate for making it to have a good electrical contact. The pellet thus prepared is placed between two electrodes of a specially designed sample holder and placed in a heater controlled by a controller. The sample is heated till the temperature of the furnace reaches around  $800^\circ\text{C}$ - $1000^\circ\text{C}$  and later on the heater is switched off and when the sample is cooling the readings of the current conducting through the circuit is recorded from nanoammeter connected in the circuit. The cooling process is chosen for recording of the values of current as the phase identification of the sample that is from ferrimagnetic to paramagnetic phase and also the transition temperature called curie temperature can be identified. The semiconductor nature of the synthesized samples can be effectively studied during cooling process where, as the temperature of the sample decreases, the dc electrical resistivity of the sample increases which is the characteristic feature of a semiconductor since a semiconductor has negative temperature coefficient of resistance.

### XRD

**studies:** Fig(1) shows the XRD plots drawn for intensity vs diffraction angle of the samples that were prepared. The XRD plots revealed the formation of a single -phase cubic spinel structure and the data is confirmed by comparing the same with the reference data from JCPDS card number. The XRD patterns confirmed the basic crystal structure of the prepared samples. The obtained P-XRD patterns of all Gd samples show a highly pure, single-phase spinel crystal structure. The existence of characteristic peaks at  $18.24$ ,  $30.24$ ,  $35.65$ ,  $37.25$ ,  $43.22$ ,  $53.60$ , and  $57.16$  correspond to the (111) (220), (311), (222), (400), (422), (511), and (440) are considered as main lattice planes in the P-XRD patterns, which provides evidence for the development of spinel structure with  $Fd-3m$  space group.

Table 1. Structural parameters : crystallite size ( $D$ ), lattice parameter ( $a$ ), Volume ( $V$ ), X-ray density ( $d_x$ ), bulk density ( $d_B$ ), and percentage porosity ( $P\%$ ), for the synthesized Gd doped MnCd nanoferrite for various compositions of  $x$ .

In the figures given below it must benotedthat Gd-0 refers to the compound with  $x=0.000$ , Gd-1 refers to the compound with  $x=0.005$ , Gd-2 refers to the compound with  $x=0.010$ , Gd-3 refers to the compound with  $x=0.015$ , Gd-4 refers to the compound with  $x=0.020$ , Gd-5 refersto the compound with  $x=0.025$ ,

Table 1

x	FWHM	D (nm)	D- Spacing	a Å	LA	LB	dx	dB	Volume	P%
Gd-0 (0.000)	0.2614	31.95	2.4952	8.3007	3.5943	2.9348	6.29123	3.164	571.938	43.964
Gd-1 (0.005)	0.2562	32.60	2.4996	8.3154	3.6007	2.9399	6.01948	3.061	574.975	40.492
Gd-2 (0.010)	0.2483	33.62	2.5046	8.3320	3.6079	2.9458	6.25023	3.112	578.428	39.580
Gd-3 (0.015)	0.2433	34.30	2.5104	8.3510	3.6161	2.9526	6.26307	3.145	582.410	39.014
Gd-4 (0.020)	0.2340	35.66	2.5171	8.3734	3.6258	2.9605	6.27574	3.158	587.099	38.796
Gd-5 (0.025)	0.2287	36.48	2.5235	8.3946	3.6350	2.9680	6.29097	3.162	591.568	38.741

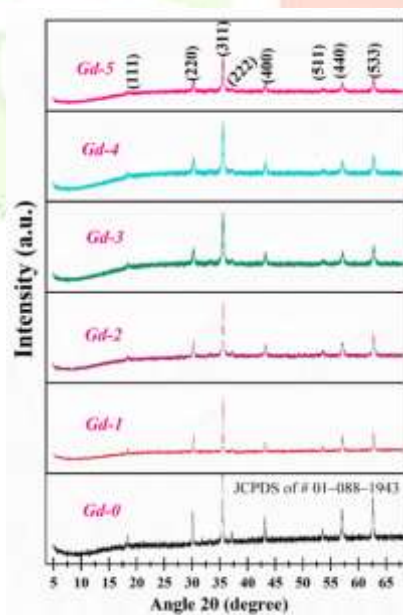


Fig. 1(a). P-XRD patterns of Gd<sup>3+</sup>-doped (Gd-0- Gd-5) nano ferrites.

From the table 1, it is observed that the lattice constant,  $a$  of the samples increases with the increase in the doping concentration and this can be attributed to the replacing of Fe<sup>3+</sup> ions by Gd<sup>3+</sup> ions as the former is larger in size than the latter. It is also observed that the average crystallite size of the samples that were prepared Mn<sub>0.3</sub>Cd<sub>0.7</sub>Gd<sub>x</sub>Fe<sub>2-x</sub>O<sub>4</sub> of different compositions and calculated using Debye-scherrer's formula

was found in the range of 32-36nm. The other crystal parameters that include lattice parameter also found to increase with the increase in the concentration of doping and obeys Vegard's law.

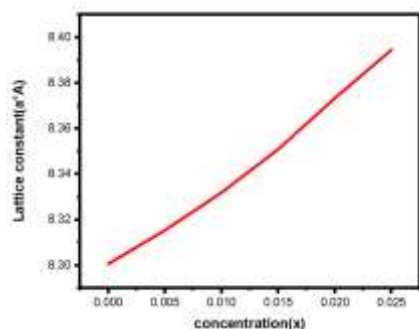
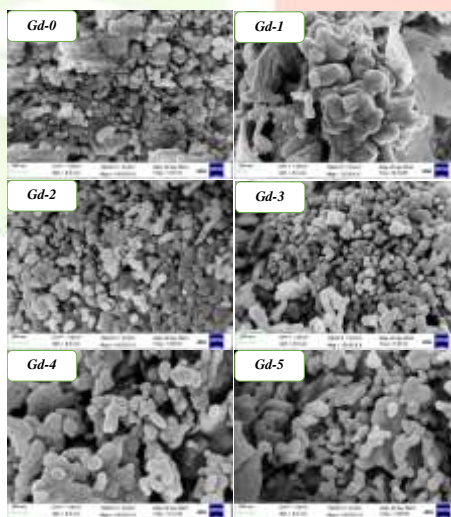


Fig.1(b) Graph using Vegard's Law

From the above graph it is observed that as the doping concentration is increased the lattice parameter also increases. The law assumes a linear relationship between the lattice parameter and the composition.

The hopping lengths that were calculated using equations (3a) and (3b) were found to increase as hopping length is directly proportional to 'a' the increase in the lattice constant is due to the larger ionic radius of  $Gd^{3+}$  ion (0.9 Å) compared to those of  $Mn^{3+}$  ion and  $Fe^{3+}$  ion (0.64 Å) [ ] where in the substitution of  $Fe^{3+}$  ions by  $Gd^{3+}$  results in the increase in the size of the lattice which is explained earlier.

**FESEM & EDAANALYSIS:** Field Emission Scanning Electron Microscopy is a high resolution imaging characterization technique that is used to study the surface morphology and composition of materials. FESEM uses a focussed beam of electrons to scan the surface of the chosen samples thereby producing a high resolution images and spectroscopic data which are analyzed to extract information about the sample's surface morphology, composition and properties. The surface particle size of the pure and Gd-doped ferrite sample was approximately estimated to be between 22.23-34.26 nm, which is in close agreement with the crystallite size ( $D_{P-XRD}$ ) value found through P-XRD analysis (Scherrer's method) for the same sample. The observed average grain size proved the nanocrystalline structure of the prepared samples. The purported chemical purity of all Gd-system-prepared materials is confirmed by the identified EDX spectrum, which only displays the peaks of Mn, Cd, Gd, iron(Fe), and oxygen(O).



Fig(2): FESEM Micrographs of Gd doped MnCd nanoferrites

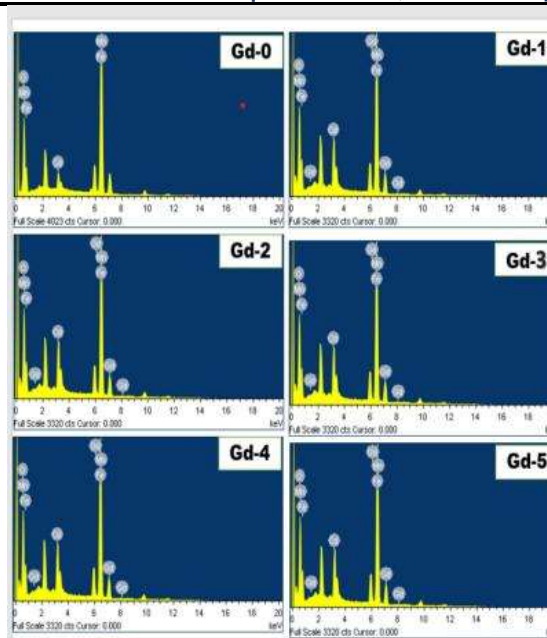


Fig. 3. EDX photographs of pristine (Gd-0) and  $Gd^{3+}$ -doped (Gd-1- Gd-5) nanoferrites

**HRTEM ANALYSIS:** HRTEM is a characterization technique that is used to determine crystal structures. The images show a lattice resolved image of the nanoferrites with a clear arrangement of atoms. The image has distinct lattice fringes that indicate a high degree of crystallinity. The interplanar spacing is measured to be approximately 0.25 nm, corresponding to the (311) plane of the cubic spinel structure. The HRTEM image confirms the cubic spinel structure. They have a size range of approximately 22-26 nm and exhibit decreasing particle size behavior as the  $Gd^{3+}$  content increases.

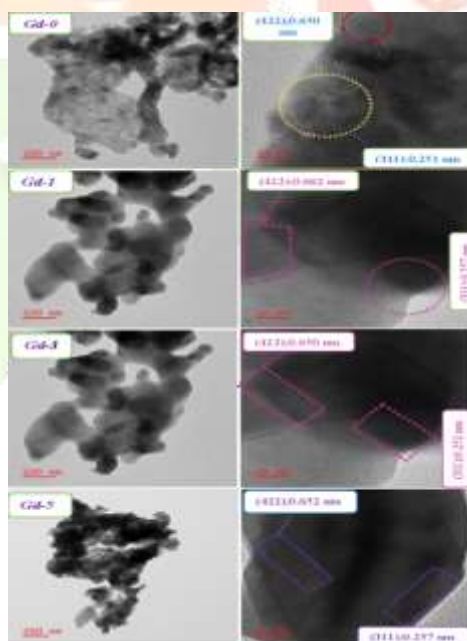
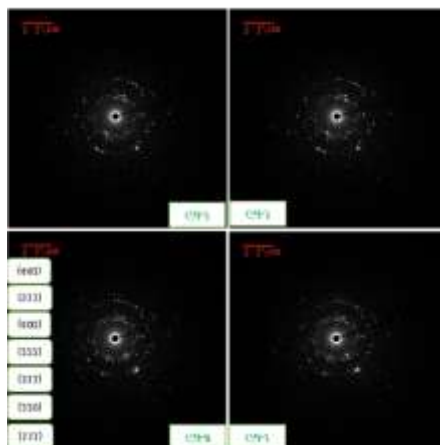


Fig. 4. HRTEM micrographs of  $Mn_{0.3}Cd_{0.7}Gd_xFe_{2-x}O_4$  nanoparticles (a) Gd-0, (b) Gd-1, (c) Gd-3, (d) Gd-5.

**SAED ANALYSIS:** It is a characterization technique used to study the crystal structure of materials. A diffraction pattern is produced from a selected area of the sample. The sharp spots in the diffraction pattern indicate a crystalline material and the concentric rings indicate a polycrystalline material. The SAED pattern indicates a cubic spinel structure. The below figure confirms the above analysis.



**Fig. 5. SAED patterns for  $Mn_{0.3}Cd_{0.7}Gd_xFe_{2-x}O_4$  ( $x= 0.000$  for Gd-0, 0.0005 for Gd-1, 0.015 for Gd-3 and 0.025 for Gd-5) nanoparticles**

*Diffraction rings relate to the  $Fd-3m$  space group's (111), (220), (311), (222), (400), (440), and (511), planes.*

**FTIR ANALYSIS:** This characterization technique involves measuring the absorption of infrared radiation by the nanoferrite samples. On analysis of FTIR spectrum, the chemical composition, crystal structure and surface properties and the Gd doping in the MnCd nanoferrites are known.

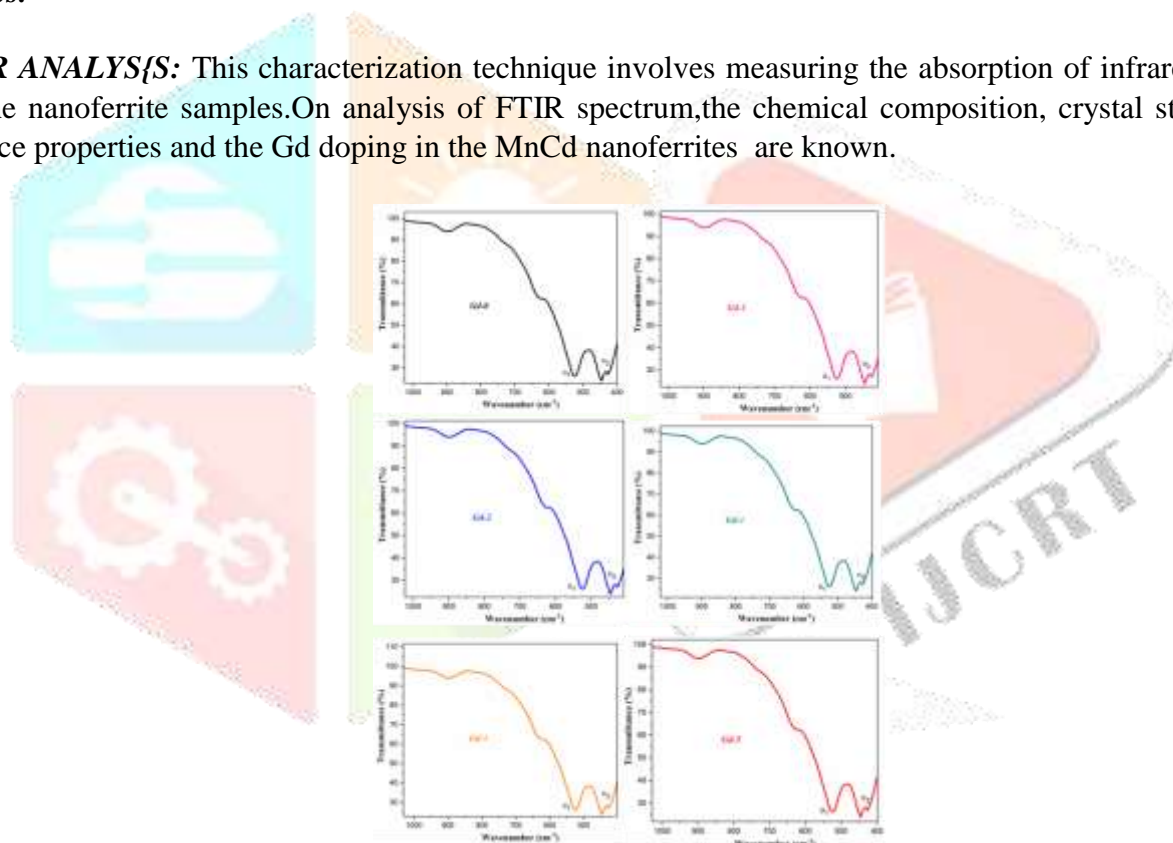


**Fig. 6 FTIR transmission spectra of  $Mn_{0.3}Cd_{0.7}Fe_{2-x}Gd_xO_4$  ( $x= Gd-0$  to  $Gd-5$ ) ferrite nanoparticles.**

**Metal -oxygen Bonds:** The peaks in the range 400-600 $cm^{-1}$  indicate the bond vibrations of Mn-O, Cd-O and Gd-O. FTIR confirms the presence of Mn, Cd, and Gd in the nanoferrites.

- The vibration of metal-oxygen group complexes in the octahedral B-site is responsible for the lower frequency bands  $\nu_2$   $cm^{-1}$ . Peaks in this range indicate B site occupancy by metal ions,
- Trivalent metal-oxygen ( $Fe^{3+}-O^{2-}$ ) bond stretching vibration in the tetrahedral A-site is associated with the higher frequency band  $\nu_1$   $cm^{-1}$ . Peaks in this range indicate B site occupancy by metal ions,
- FTIR determines the distribution of metal ions between A and B sites.

**DC Resistivity** :The procedure followed for the study of dc electrical resistivity which is temperature dependent involves making a pellet form of the sample prepared using hydraulic press and then the pellet is coated with silver paint on both of its surfaces and heated on a hot plate for making it to have a good electrical contact.The pellete thus prepared is placed between two electrodes of a specially designed sample holder and placed in a heater controlled by a controller. The sample is heated till the temperature of the furnace reaches around 800°C and later on the heater is switched off and when the sample is cooling the readings of the current conducting through the circuit is recorded from nanoammeter connected in the circuit.The cooling process is chosen for recording of the values of current as the phase identification of the samole in the pellet form that is ferrimagnetic to paramagnetic phase and also the transition temperature called curie temperature can be identified..The semiconductor nature of the synthesized samples can be effectively studied during cooling process where, as the temperature of the sample decreases, the dc electrical resistivity of the sample increases which is the characteristic feature of a semiconductor since a semiconductor has negative temperature coefficient of resistance. During the process a constant dc voltage of 2.5V is maintained across the sample. The value of the current is noted for every 5°C .decrease in temperature.The value of Resistance ,R is detemined usinf the relation  $R=V/I$ ------(7)

The DC resistivity ,  $\rho$   $\sigma$  of the sample is determined using the formula

$$\text{pellet } \rho = R \cdot A / L \text{ -----(8)}$$

Where A is the cross sectional area and L is the length between the electrodes.

**Resistivity-Temperature plot:**The graph is plotted between DC resistivity and temperature for various concentrations of the doping for  $x=0.000,0.005,0.010,0.015,0.020,0.025$  and is as shown in the Fig(10)

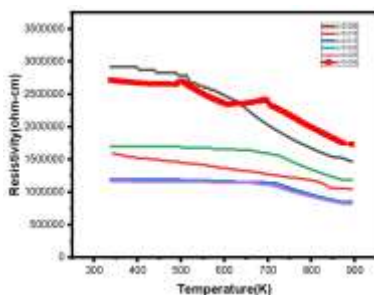
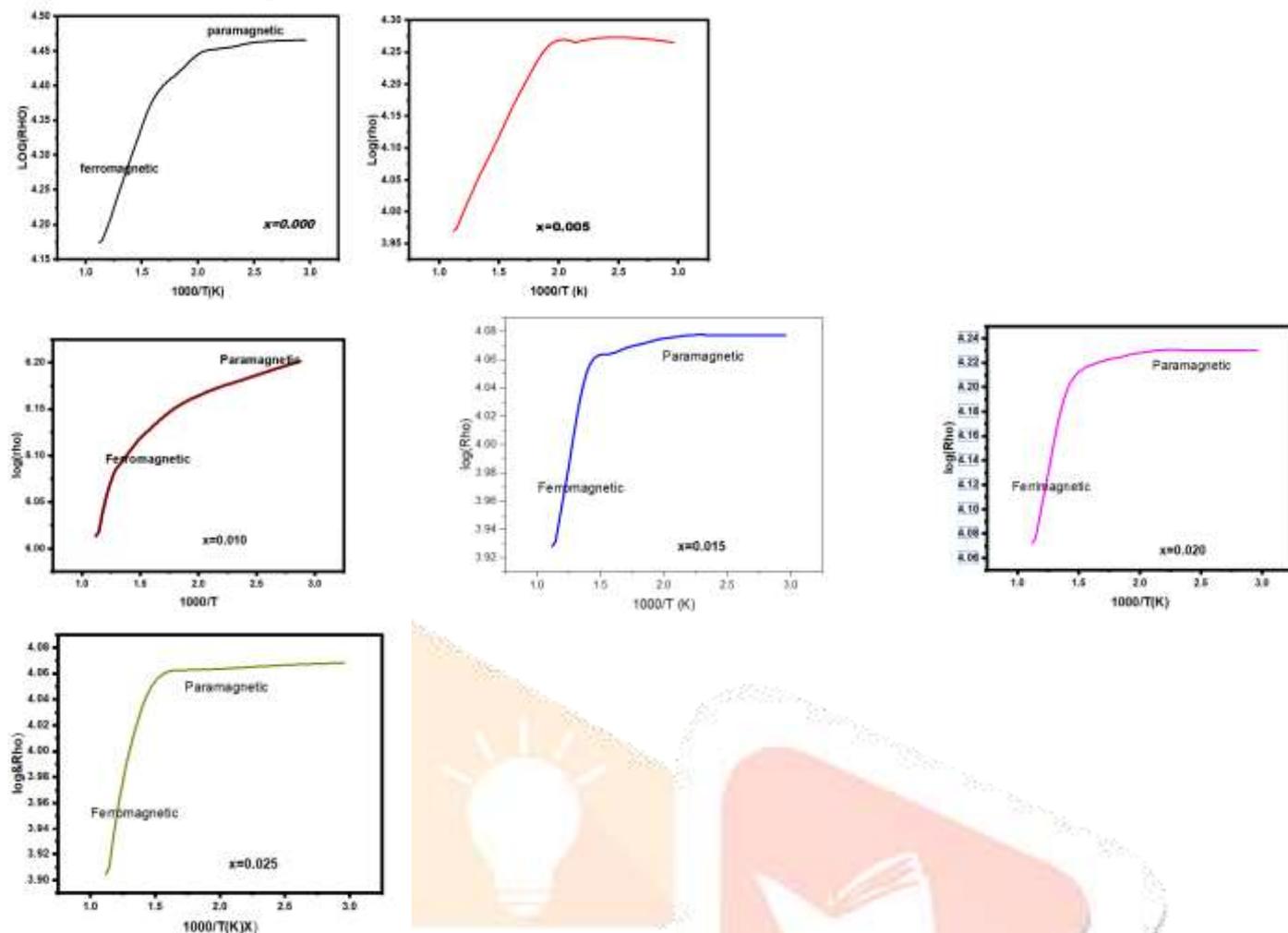


Fig.10.Temperature dependence of dc electrical resistivity of  $Mn_{0.3}Cd_{0.3}Gd_xFe_{2-x}O_4$  ( $x=0.000,0.005,0.010,0.015,0.020,0.025$ ) nanoparticles.

From the graph it is evident that the value of resistivity decreases with the increase in the temperature for the samples of various concentrations.The semiconducting nature of the prepared samples is known visibly.Also the increase in the doping concentrations decreases the resistivity values.

Log( $\rho$ ) Vs 1000/T plots

Fig(11) Log( $\rho$ ) Vs 1000/T plots of Gd doped MnCd nanoferrites for  $x=0.000,0.005,0.010,0.015,0.020,0.025$

The plots drawn above refers to Arrhenius plots which help in analyzing the electrical resistivity ( $\rho$ ) as a function of Temperature.

The plots show a rapid decrease in the values of resistivity with the increase in the temperature. This indicates increased conductivity, magnetic moments aligning, reducing scattering and increasing mobility and this behaviour is observed in the ferrimagnetic region which is the typical characteristic of ferrimagnetic materials.

At Curie temperature the transition of the material from ferrimagnetic to paramagnetic occurs. The curve flattens out indicating transition to a paramagnetic state where magnetic moments are randomly aligned. The resistivity becomes relatively constant as magnetic properties no longer dominate electronic behaviour. Moreover this constant behaviour in the paramagnetic region suggests that the electronic properties of the material samples are more stable with reduced influence from magnetic interactions. The Inflection point is the point on the curve where it changes from increasing values to a constant behaviour indicating the onset of paramagnetic state.

The samples of gadolinium doped manganese cadmium nanoferrites exhibits strong ferrimagnetic behaviour at lower temperatures, with rapid changes in resistivity. The transition to a paramagnetic state at Curie Temperature ( $T_c$ ) indicates a loss of magnetic order, leading to more stable electronic properties.

The plots provide valuable information about the material's magnetic and electronic properties, useful for understanding its behaviour in various applications.

The activation energy ( $E_a$ ) is determined for the samples for various concentrations of doping. It was observed that the values of  $E_a$  were found to decrease with increasing doping concentrations indicating improved electrical conductivity. The lowest  $E_a=0.00713\text{eV}$  for  $x=0.020$  suggests optimal electrical conductivity. However, at a higher doping concentration of  $x=0.025$ ,  $E_a$  increases to  $0.01114\text{eV}$  indicating a decrease in electrical conductivity. The reason attributed for the initial decrease in  $E_a$  can be due to the increase in the number of charge carriers due to the doping of  $\text{Gd}^{3+}$ . The increase in  $E_a$  at higher doping concentration of  $x=0.025$  could be due to over doping, leading to a decrease in charge carrier mobility and can be due to electrical conductivity of crystal structure that causes a reduction in electrical conductivity.

The band gap energy,  $E_g$  of the mentioned samples of Gadolinium doped Manganese cadmium nanoferrites is calculated from the activation energy,  $E_a$ . The band gap energy is the energy difference between the valence and the conduction bands,  $E_g$  and  $E_a$  are related by the relation

$$E_g = 2E_a \text{ (approximately) } \text{-----(9) ( according to Mott's formula)}$$

The Conductivity,  $\sigma$ , can be calculated by using the formula

$$\sigma = \sigma_0 \times \exp(-E_a/k_B T) \text{-----(10)}$$

Where  $\sigma$  is the Conductivity

$\sigma_0$  is the pre exponential factor and is approximately equal to 1

$E_a$  is the activation energy

$k_B$  is Boltzmann constant equal to  $8.617 \times 10^{-5} \text{ eV/K}$

$T$  is the temperature in Kelvin

The values of  $E_g$  for various concentrations of the dopant which is rare earth metal ion  $Gd^{+9}$

is calculated at transition temperature and the values are tabulated in the Table 2.

Table 2: Curie temperature values, Activation energy values and Resistivity values at curie temperature and at maximum temperature

S.No	Concentration of Gd dopant(x)	Curie Temperature Tc (K)	Activation Energy (Ea) eV	Resistivity at Tc (ohm-cm)	Resistivity at T=893K (ohm-cm)	Energy band gap( $E_g$ ) eV
1	0.000	461.52	0.00452	2832151	1470962	0.0904
2	0.005	471.07	0.02266	2640172	1760115	0.04532
3	0.010	433.15	0.00210	1503826	1048887	0.00420
4	0.015	497.15	0.00865	1194217	855855.9	0.01730
5	0.020	472.93	0.00713	1699463	1188243	0.01426
6	0.025	395.25	0.01114	1158667	828892.5	0.02228

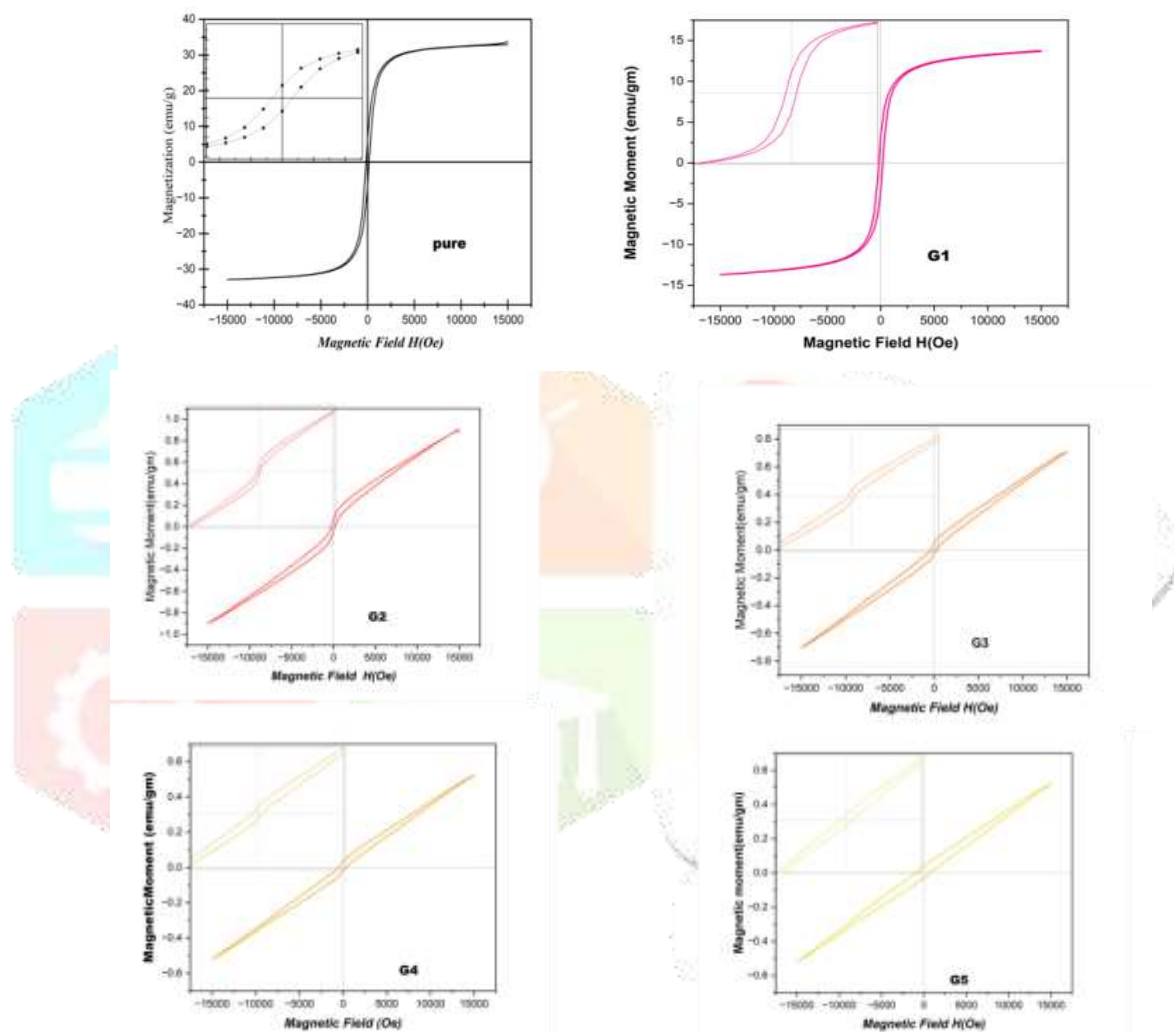
From the values of  $E_g$  it is observed that there is a narrow band gap that makes it easier for electrons to move between valence band and conduction band and the samples exhibit semiconducting behaviour. Also the relatively small band gap energy indicates p-type semiconducting behaviour, where holes which are positive charge carriers dominate the conductivity of the samples that are synthesized. The pure or undoped MnCd nanoferrite has an  $E_g$  approximately equal to 0.1eV, for the doping concentration  $x=0.005, 0.015, 0.020$   $E_g$  value has decreased, but for  $x=0.010$ , the value of  $E_g$  is very small and the reason to be considered is thermal energy at the transition temperature that can excite electrons and causes a decrease in the value of  $E_g$ . Further it must be noted that at higher temperature of 893K,  $E_g$  is calculated to be 0.166eV. For  $x=0.025$ , there is a slight increase which could be due to saturation of dopant concentration.

**VSM ANALYSIS:** Vibrating Sample Magnetometry is a characterization technique used to measure the magnetic properties of materials. The magnetic moment ( $m$ ) of the sample as a function of the applied magnetic field ( $H$ ). The graph is plotted between  $m$  vs  $H$  to obtain the magnetization curves.

The plots shows a very narrow width and these are a characteristic feature of soft ferrites. The S shape indicates a rapid increase in magnetization with applied field, followed by saturation

Which is the typical behavior of soft magnetic materials. Gadolinium doped Mn Cd nanoferrites are a type of soft ferrite material and the doping of  $Gd^{3+}$  ions can enhance the magnetic properties of the samples. From the magnetic properties of Magnetic Saturation,  $M_s$ , and Coercivity,  $H_c$ , it was observed that the samples that are synthesized had low  $M_s$  and high  $H_c$  and the reasons attributed are Doping Effects where the doping of Gd can lead to a reduction in  $M_s$  due to the substitution of magnetic ions (Mn, Cd) with the non magnetic Gd ions and also due to surface effects such as spin canting or surface anisotropy and Mn-Cd ratio and cation distribution.

**Hysteresis Loops:** The magnetization curves are obtained by plotting between magnetic moment and magnetizing field.



Fig(12) M-H magnetization curves of Gd doped Mn-Cd nanoferrites

Accordingly, as demonstrated by Figs. 12, the M-H (magnetization field) loops of produced  $Mn_{0.3}Cd_{0.7}Gd_xFe_{2-x}O_4$  nanoferrites have been determined at room temperature (300 K) using a magnetic field applied within the range of  $\pm 20$  kOe.

As seen in Fig. 12. G0(pure) to G5, samples exhibited insufficient ferrimagnetic behavior with remanences and coercive fields and all synthesized samples suggests the presence of a saturated superparamagnetic component.

Table 3 : Calculated values of coercivity ( $H_c$ ), remanence (MR), magnetic saturation ( $M_s$ ), anisotropy constant (K), and squareness (S), and determined initial permeability for synthesized  $Mn_{0.3}Cd_{0.7}Gd_xFe_{2-x}O_4$  nanoferrites ( $x = 0.000, 0.005, 0.010, 0.015, 0.020, 0.025$ )

In the VSM analysis it must be noted that the samples of Gadolinium doped manganese cadmium nanoferrites are labelled as pure, G1, G2, G3, G4, G5 and these denote the doping concentrations as given that is pure denotes a sample with no doping i.e.,  $x=0.000$ , G1 represents for  $x=0.005$ , G2 for  $x=0.010$ , G3 for  $x=0.015$ , G4 for  $x=0.020$  and finally G5 = 0.025.

TABLE SHOWING VALUES OF MAGNETIC PARAMETERS							
Gd series							
Sno	COMPOSITION OF Gd	MAGNETIC SATURATION(emu/gm)	RETENTIVITY(emu/gm)	COERCIVITY(Oe)	MAGNETIC ANISOTROPY CONSTANT(K)	BOHR MAGNETON	SQR
1	0	33.7085	6.6147	166.5695	5729.395909	1.634786806	0.1962324
2	0.005	13.657	3.79315	160.784	2240.639886	0.663573701	0.277744
3	0.01	0.8796	0.06474	179.379	161.0018045	0.04286227	0.0736016
4	0.015	0.688624	0.06061	177.01	124.3809533	0.03358426	0.0880161
5	0.02	0.51737	0.03248	392.133	207.0182145	0.025279152	0.0627791
6	0.025	0.520939	0.036049	595.002	316.285456	0.025500827	0.0692

The observed decrease in Magnetic Saturation ( $M_s$ ) with increase in the doping concentration of three rare earth metal ion,  $Gd^{3+}$ , can be attributed to the alteration of magnetic moments and interactions within the material. When  $Gd^{3+}$  ions are introduced into the pure crystal lattice, these ions disrupt the magnetic ordering leading to a significant reduction in  $M_s$ .

From the table showing the values of magnetic retentivity with doping concentration being increased, it is observed that for the pure sample without doping, the value of  $M_r$  is the highest value which means the pure form can retain a significant amount of magnetization and hence magnetic properties. As the dopant is added that is  $x=0.005$ , the  $Gd^{3+}$  ions disrupt the magnetic ordering and this continued for  $x=0.010, 0.015$  and for  $x=0.020$  and  $0.025$ , there is a slight increase in the value due to reorientation of magnetic moments which indicates that at doping concentrations of  $0.020, 0.025$ , the material adapts to the dopant ions.

The Coercivity values are found to increase with the increase in the doping concentration as the dopant ions are enhancing the resistance of the samples that are synthesized to demagnetization. It is observed that Magnetic Saturation ( $M_s$ ) is decreasing while Coercivity ( $H_c$ ) is increasing with the increase in the concentration of doping and this infers that the Gd ions are likely disrupting the alignment of magnetic moments which leads to a decrease in  $M_s$ . Also the Gd ions are pinning the domain walls and making harder for the ions to move and reverse the magnetization which causes an increase in  $H_c$  and hence makes the material more resistant to demagnetization and these are some interesting properties of the designed samples.

The retentivity is found to decrease with the increase in the concentration of the Gd ions due to non-magnetic Gd ions being substituted for magnetic Mn-Cd ions, reducing the net magnetic moment.

Magnetic Anisotropy decreases with the increase in the dopant concentration initially due to random substitution of Gd ions that disrupts magnetic ordering and increased surface effects and for  $x=0.020, 0.025$  there is a slight increase in anisotropy due to increased Gd-Gd interactions.

The decrease in the magnetic anisotropy indicates a reduction in the magnetic moment with the increasing Gd doping concentration and this is due to the changes in the crystal structure, magnetic interactions and spin alignment.

The initial increase in the Squareness ratio indicates improved squareness of the hysteresis loop probably due to enhanced magnetic interactions for  $x=0.000, 0.005$ . The rapid decrease at  $x=0.010$  indicates a loss of squareness due to the disruption of the magnetic ordering. The low and steady values at higher concentrations is probably due to the dominant effect of Gd ions. Thus the magnetic properties of the samples are studied.

**CONCLUSION :** The structural, electrical and magnetic properties are thus studied and investigated for the  $Mn_{0.3}Cd_{0.7}Gd_xFe_{2-x}O_4$  nanoferrites and can find their use in applications such as Magnetic Resonance Imaging (MRI) contrast agents, Magnetic Hyperthermia (heat inducing agents), Magnetic sensors, Magnetic storage devices, Biomedical applications, Catalysis, Magnetic Fluids, Electromagnetic interference shielding, Spintronics and many more. The small band gap of the synthesized samples which is  $<1.0eV$  is suitable in applications that include infrared detectors, thermoelectric devices and some solar cells.

**References**

- [1] A. Mahesh Kumar, M. Chaitanya Varma, Charu Lata Dubey, K. H. Rao, S. C Kashyap J. Magn. Mater. **320**, 1995 (2008).
- [2] R. N. Bhowmik, R. Ranganathan Solid State Commun. **141**, 365(2007).
- [3] R. F. Soohoo, Theory and Applications of Ferrites Englewood Cliffs, NJ: Printice-Hall (1960) p. 24.
- [4] A. Lakshman, K. H. Rao, R. G. Mendiratta J. Magn. Mater. **250**, 92 (2002).
- [5] K. H. Rao, N. K. Gaur, K. Aggarwal, R. G. Mendiratta J. Appl. Phys. **53**, 1122(1982).
- [6] B. D. Cullity, S. R. Stock "Elements of X-ray diffraction", third Ed. Prentice-Hall Inc. New Jersey (2001) p.388.
- [7] J. M. Daniels, A. Rosenwaig Can. J. Phys. **48**, 381 (1970).
- [8] L. K. Leung, B. J. Evans, A. H. Morrish Phys. Rev. B **8**, 29 (1973).
- [9] A. Mahesh Kumar, K. H. Rao, J. M. Greneche J. Appl. Phys. **105**, 073919 (2009).
- [10] R. Laishram, S. Phanjobam, H. N. K. Sarma, Chandra Prakash J. Phys. D: Appl. Phys. **32**, 2151 (1999).
- [11] K. P. Chae, Y. B. Lee, J. G. Lee, S. H. Lee J. Magn. Mater. **220**, 59 (2000).
- [12] S. H. Lee, S. J. Yoon, G. J. Lee, H. S. Kim, C. H. Yo, K. Ahn, D. H. Lee, K. H. Kim Mater. Chem. Phys. **61**, 147 (1999).
- [13] K. P. Chae, Y. B. Lee, J. G. Lee, S. H. Lee J. Magn. Mater. **220**, 59 (2000).
- [14] A. M. Abdeen, J. Magn. Mater. **192**, 121 (1999).
- [15] C. N. Chinnasamy, A. Narayanasamy, N. Ponpandian, K. Chattopadhyay, K. Shinoda, B. Jayadevan, K. Tohji, K. Nakatsuka, T. Furubyashi, I. Nakatani Phys. Rev. B **63**, 184108(2001).
- [16] N. Ponpandian, P. Balaya, A. Narayanasamy J. Phys: Condens. Matter. **14**, 3221 (2002).
- [17] A. Verma, O. P. Thakur, C. Prakash, T. C. Goel, R. G. Mendiratta Mater. Sci. & Engg. B **116**, 1 (2005).
- [18] H. Su, H. Zhang, X. Tang, Y. Jing, Y. Liu J. Magn. Mater. **310**, 17 (2007).
- [19] A. Verma, T. C. Goel, R. G. Mendiratta J. Magn. Mater. **210**, 274 (2000).
- [20] S. Zahi, M. Hashim, A. R. Daud, J. Magn. Mater. **308**, 177 (2007).
- [21] D. Condurache, C. Pasnicu, E. Luca "International Conference on Ferrites", ICF – **4**, 157 (1985).
- [22] R. V. Mangalaraja, S. Thomas Lee, S. Ananthakumar, P. Manohar, Carlos P. Camurri Mater. Sci. Eng. A **476**, 234 (2008).
- [23] J. Smit, H. P. J. Wijn "Ferrites" Philips Technical Library, Eindhoven (1959) 244.
- [24] B. P. Rao, K. H. Rao J. Magn. Soc. Jpn. **22**, 305 (1998).